CrossMark

RESEARCH ARTICLE

Development and application of three-dimensional potential source contribution function (3D-PSCF)

In Sun Kim[1] · Daehyun Wee[1] · Yong Pyo Kim[1,2] · Ji Yi Lee[3]

Abstract A potential source contribution function (PSCF) can indicate the source areas of high air pollutant concentrations using backward trajectories. However, the conventional two-dimensional PSCF (2D-PSCF) cannot consider the emission and transport height of air pollutants. That missing information might be critical because injection height varies depending on the source type, such as with biomass burning. We developed a simple algorithm to account for the height of trajectories with high concentrations and combined it with the conventional PSCF to devise 3D-PSCF. We demonstrate the applicability of the 3D-PSCF by applying it to particulate PAH data collected from September 2006 to August 2007 in Seoul. We found variation in the results from 3D-PSCF with threshold heights from 3,000 to 1,500 m. Applying 2,000 m as the threshold height in the PSCF calculation most clearly determined the possible source areas of air pollutants from biomass fuel burning that were affecting the air quality in Seoul.

Responsible editor: Marcus Schulz

Highlights Injection height of air pollutants cannot be considered in the conventional PSCF
Injection heights differ depending on source types, such as with biomass burning
The proposed 3D-PSCF accounts for the height of trajectories
Possible source areas for biomass burning were more clearly determined using 3D-PSCF

✉ Daehyun Wee
 dhwee@ewha.ac.kr

[1] Department of Environmental Science and Engineering, Ewha Womans University, 52, Ewhayeodae-gil, Seodaemun-gu, Seoul 03760, Korea

[2] Department of Chemical Engineering & Materials Science, Ewha Womans University, 52, Ewhayeodae-gil, Seodaemun-gu, Seoul 03760, Korea

[3] Department of Environmental Engineering, BK21 Team for Biohydrogen Production, Chosun University, 309, Pilmun-daero, Dong-gu, Gwangju 61452, Korea

Introduction

Trajectory analysis has been widely used to investigate the transport process of air pollutants and to figure out source areas that affect the air pollution at receptor areas, especially on the regional or interregional scale. To deal with large sets of trajectories, a variety of statistical analysis methods have been developed and applied, such as flow climatology, cluster analysis, residence time analysis and conditional probability, concentration fields, redistribution concentration fields, and inverse modeling (Stohl 1998). Tian et al. (2015, 2016) developed new methods, source directional apportionment (SDA) and source regional apportionment (SRA), to determine source transport and regional contribution quantitatively in China based on the trajectory analysis.

The potential source contribution function (PSCF) is a trajectory analysis method based on the concept of conditional probability (Ashbaugh et al. 1985; Malm et al. 1986). PSCF can indicate a potential source region contributing to a high air pollutant concentration by using the total number of trajectories over a given geographic region and the number of trajectories with a high air pollutant concentration at the receptor

(Ashbaugh et al. 1985). It has been used in several studies on transport of many kinds of air pollutants (Zeng and Hopke 1989; Cheng et al. 1993a, b, 1996; Gao et al. 1993, 1994, 1996; Fan et al. 1995). Heo et al. (2009) used PSCF to figure out possible source areas contributing to elevated secondary particle concentrations (sulfate and nitrate) in Seoul. Nguyen et al. (2015) evaluated the influences of long-range-transported smoke plumes on the highly elevated OC concentrations measured at Gosan, a background site in Korea, using PSCF. Several researches applied PSCF for ambient particulate matters in China (Wang et al. 2004, 2006; Zhang et al. 2011). Several techniques have been developed and applied to reduce the uncertainty in PSCF, for example a weighting function and total PSCF (Hopke et al. 1995; Cheng et al. 1993b).

Biomass burning is a significant source of air pollution in Northeast Asia (Streets and Yarber 2003). There are several types of biomass burning such as residential burning for heating and cooking (biofuel burning), open burning after harvest, and forest fires. The injection height varies depending on the type of biomass burning; at the surface level for residential burning and at the atmospheric boundary layer level (500–3,000 m) in the mid-Korean peninsula (Choi et al. 2008) for open burning. The injection height from forest fires varies depending on the intensity of the fire. For some forest fires in Siberia in spring, researchers used a simulated vertical level of up to 5 km as the injection height in their modeling study based on the study results in the USA (In and Kim 2010). On the other hand, the injection heights from small open burning could be lower than it from forest fire because of lower heat flux released from small fire.

Polycyclic aromatic hydrocarbons (PAHs) are a class of compounds containing carbon and hydrogen with a fused ring structure containing at least two benzene rings. These compounds are widely distributed in the atmosphere and highly carcinogenic to humans. PAHs are mostly formed during the incomplete combustion and pyrolysis of fossil fuels or wood and from the release of petroleum products. Anthropogenic sources of PAHs are power plants, industrial, and domestic combustion, transportation, coke ovens, and biomass burning (Ravindra et al. 2008).

The ratio of each PAH species varies with combustion conditions such as fuel type and combustor temperature. That is, each specific emission source has a characteristic PAH composition profile. Therefore, particulate PAHs are suitable for receptor modeling (Marr et al. 2006; Lee and Kim 2007). Venturini et al. (2014) identified source contributions of air pollutants including PAHs subjected by positive matrix factorization (PMF) and examined if sources are local or regional among wind direction. Still, in the current PSCF analysis studies, all kinds of biomass burning are treated as one (see, for example, Kim et al. 2013). In other words, the conventional PSCF does not consider the injection height of air pollutants.

To differentiate the effects of these, we developed a new method, the three-dimensional potential source contribution function (3D-PSCF), and demonstrated its applicability. First, we developed a simple algorithm to account for the height of a trajectory with a high pollutant concentration in the PSCF. Then, we applied the developed 3D-PSCF to the measurement of particulate PAHs in Seoul to consider the differences of biofuel burning and small open burning from large open burning and forest fires. In doing so, we more clearly identified the emission areas for biofuel burning and small open burning.

Development of 3D-PSCF

Because 3D-PSCF is based on the conventional or 2D-PSCF, we first present the basic algorithm of the 2D-PSCF and explain its characteristics including limitations. Then we present the 3D-PSCF algorithm.

Conventional PSCF (2D-PSCF) and limitations

The PSCF value at each cell on a PSCF plot is the ratio between how often air parcels pass through the corresponding cell and how frequently the air parcels passing through the cell are associated with polluted air at the receptor site. Cells with high PSCF values have a high possibility of containing emission sources. We briefly introduce the 2D-PSCF method in this section for ease of reference. The description given here largely follows the work of Hopke et al. (1993).

Let N be the total number of trajectory segment endpoints during the whole study period, T. If n segment trajectory endpoints fall into the ijth cell (represented by n_{ij}), the probability of this event, A_{ij}, is given by

$$P[A_{ij}] = \frac{n_{ij}}{N} \tag{1}$$

Where $P[A_{ij}]$ is a measure of the residence time of a randomly selected air parcel in the ijth cell relative to the time period T.

Suppose the same ijth cell contains a subset of m_{ij} segment endpoints for which the corresponding trajectories arrive at a receptor site when the measured pollution concentrations are higher than a pre-specified criterion value. In this study, we used the calculated mean values for each species at each site as the criteria values. The probability of this high concentration event, B_{ij}, is given by $P[B_{ij}]$,

$$P[B_{ij}] = \frac{m_{ij}}{N} \tag{2}$$

Like $P[A_{ij}]$, this subset probability is related to the residence time of an air parcel in the ijth cell, but the probability B is for contaminated air parcels.

The potential source contribution function (PSCF) is defined as

$$P_{ij} = \frac{P[B_{ij}]}{P[A_{ij}]} = \frac{m_{ij}}{n_{ij}} \qquad (3)$$

P_{ij} is the conditional probability that an air parcel that passed through the ijth cell had a high pollution concentration upon arrival at the trajectory endpoint. That is, P_{ij} is the probability value showing the related source is located in the ijth cell and, thus, does not have unit.

The conventional PSCF analysis has several limitations. For instance, when a map grid cell contains too few trajectories, most of which are associated with poor air quality at the receptor site, the cell could exhibit an exceptionally high PSCF value that is statistically invalid because of the uncertainty associated with the small number of trajectory samples. To address such a problem, other researchers have used approaches with a weighting function (Zeng and Hopke 1989; Cheng et al. 1993a; b). However, we did not use a weighting function here because we wanted to evaluate the results of our new algorithm without the influence of other modification.

Another limitation is that the conventional PSCF cannot distinguish trajectories passing through at different altitudes. We define the injection height of a pollutant as the height up to which the pollutant can penetrate the atmosphere. Air pollutants emitted from a ground-based source are known to be diffused and well mixed within the boundary layer whose thickness is normally 1 or 2 km (Wallace and Hobbs 2006; Labonne et al. 2007). Altitude studies have shown that the air pollutants emitted from forest fires can be injected into the atmosphere above 2 km (Mazzoni et al. 2007; Labonne et al. 2007; Freitas et al. 2007). On the other hand, injection height of air pollutants emitted over cropland were usually below 1 km (Martin et al. 2010; Jian and Fu 2014). Thus, the injection height depends on the source, the transport characteristics of the pollutant, and the prevailing weather conditions. Naturally, an air parcel passing through a cell can catch a particular pollutant only when it passes through the cell at an altitude lower than the injection height of that pollutant. The conventional PSCF analysis cannot include the effects of injection height for air pollutants emitted from different biomass burning activities. This effect of the third dimension, i.e., the effect of the injection height, is completely neglected in the traditional PSCF analysis, which is why we call it the 2D-PSCF.

3D-PSCF

To include the effect of injection height, we include a threshold altitude in the PSCF calculations. Because we consider not only the horizontal information but also the vertical influence of the injection height in our analysis, we name our method 3D-PSCF.

The primary idea of the 3D-PSCF method is illustrated in Fig. 1. As discussed previously, the conventional 2D-PSCF
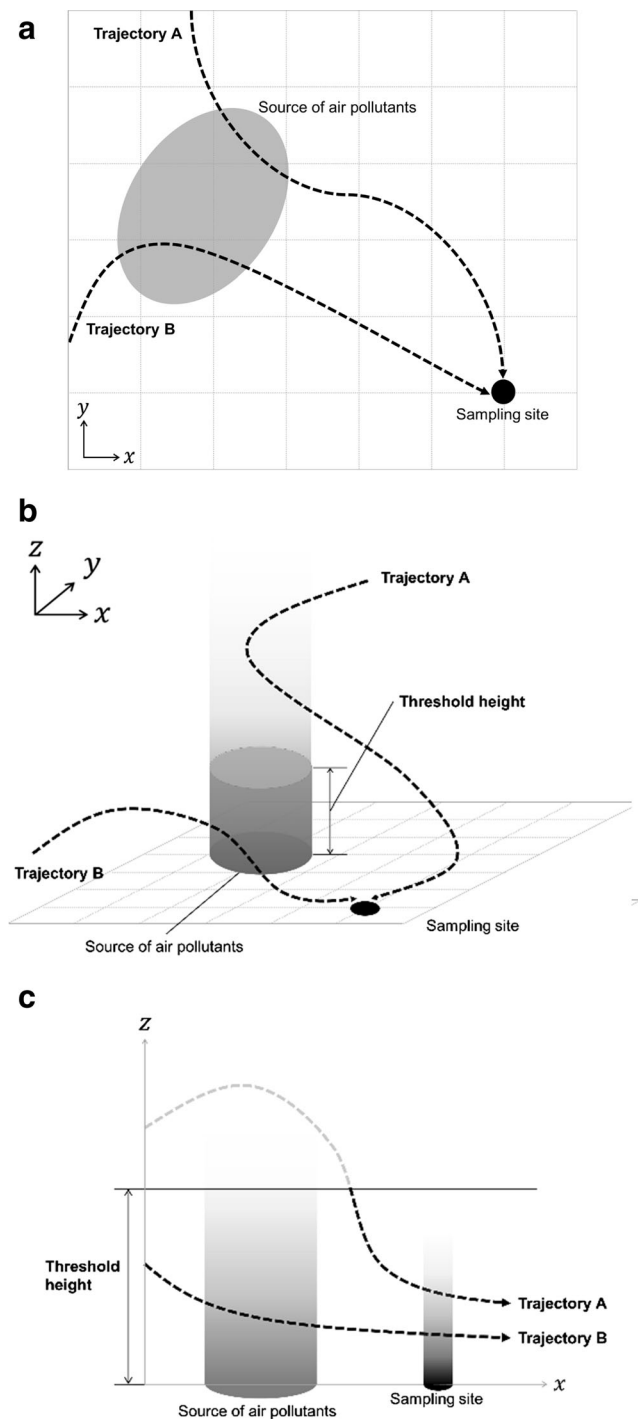

Fig. 1 Schematic illustration of the concept of (a) 2D-PSCF and (b, c) 3D-PSCF. According to the 2D-PSCF analysis, trajectory A and trajectory B have the same possibility of being contaminated by a ground source of air pollutants. The 3D-PSCF analysis distinguishes trajectory A from trajectory B. Trajectory A cannot possibly contact the pollutants from the source area because it passes above the threshold height. The part of trajectory A passing above the threshold height (gray) is not counted in the 3D-PSCF calculation. Trajectory B and the black part of Trajectory A are counted as valid because they pass below the threshold height

analysis assumes that the air parcels passing through a cell containing an emission source are indiscriminately affected by the air pollution in that cell (Fig. 1a). On the other hand, a 3D-PSCF analysis considers an air parcel passing through a cell with an emission source to be unaffected by the pollution if it passes through the cell at an altitude higher than the threshold height (Fig. 1b, c). To differentiate a trajectory going through a cell below the threshold height from one above the threshold height, we simply ignore the segment end points that lie above the threshold height during the calculation of each cell's PSCF value.

The algorithm can be summarized as follows. Let N be the total number of trajectories observed during the whole study period. If n trajectories fall into the ijth cell below the threshold height (represented by n'_{ij}) the probability of this event, A'_{ij}, is given by

$$P\left[A'_{ij}\right] \;=\; \frac{n'_{ij}}{N} \qquad (4)$$

The probability of a high concentration event, B'_{ij}, is again calculated using the threshold height.

$$P\left[B'_{ij}\right] \;=\; \frac{m'_{ij}}{N} \qquad (5)$$

where m'_{ij} trajectories pass through the ijth cell below the threshold height for which the corresponding trajectories arrive at the receptor site at a time when the measured concentration of the pollutant of interest is higher than the pre-specified critical value (typically, the median of the measured concentrations in the available data set).

The 3D-PSCF (P^{3D}_{ij}) is thus defined as

$$P^{3D}_{ij} = \frac{m'_{ij}}{n'_{ij}} \qquad (6)$$

In other words, P^{3D}_{ij} is the conditional probability that an air parcel that passes through the ijth cell below the threshold height exhibits a high concentration upon arrival at the receptor site. To evaluate the results of 3D-PSCF independently, we did not apply any other techniques to minimize the uncertainty in the PSCF calculation.

Methods

Ambient data

We collected samples at the Yongon campus of Seoul National University, Seoul, Korea (37°35′N, 127°00′E). We carried out sampling for 24 h every third day with no rain from September 2006 to August 2007. Thirteen PAH compounds were identified and quantified: Phen, Anthr, Flt, Pyr, BaA, Chry, BbF, BkF, BeP, BaP, Ind, DahA, and BghiP. The particulate PAH measurement result we used was described in detail in Lee et al. (2011).

We applied chemical mass balance (CMB) modeling to our PAH data (Jung et al. 2015). We considered seven major PAH source profiles in Table 1: coal for power plants, coke ovens and coal for residential use, gasoline and diesel vehicles, NG combustion, and biomass burning and used the contributions of biomass burning. The PAHs source profiles devised in Lee and Kim (2007) [the original references for the source profiles: coal for power plant, coke oven and coal for residential—Li et al. (2003), gasoline and diesel vehicles—Rogge et al. (1993a), NG combustion—Rogge et al. (1993b), and biomass burning—Rogge et al. (1998)]. More information about CMB modeling for PAH data is available in Lee and Kim (2007) and Kim et al. (2013).

Table 1 Source composition of individual PAH compounds in the particle phase used for source profiles (Lee and Kim 2007)

|	Coal power plant	Coal coke oven	Coal residential	Gasoline vehicle	Diesel vehicle	NG combustion	Biomass burning
Phen	0.142	0.073	0.333	0.035	0.165	0.002	0.067
Anthr	0.016	0.020	0.070	0.004	0.022	0.000	0.010
Flt	0.160	0.045	0.216	0.078	0.176	0.167	0.127
Pyr	0.140	0.079	0.085	0.098	0.305	0.161	0.166
BaA	0.099	0.112	0.044	0.075	0.049	0.090	0.066
Chry	0.191	0.120	0.064	0.149	0.134	0.436	0.247
BbF	0.073	0.129	0.064	0.114	0.039	0.052	0.063
BkF	0.015	0.084	0.030	0.078	0.036	0.071	0.069
BeP	0.061	0.111	0.025	0.078	0.035	0.021	0.047
BaP	0.035	0.101	0.034	0.075	0.018	NA	0.068
Ind	0.025	0.038	0.018	0.018	ND	NA	0.013
DahA	0.005	0.016	NA	0.013	ND	NA	0.007
BghiP	0.039	0.071	0.016	0.184	0.022	NA	0.052

NA not analyzed, *ND* not detected
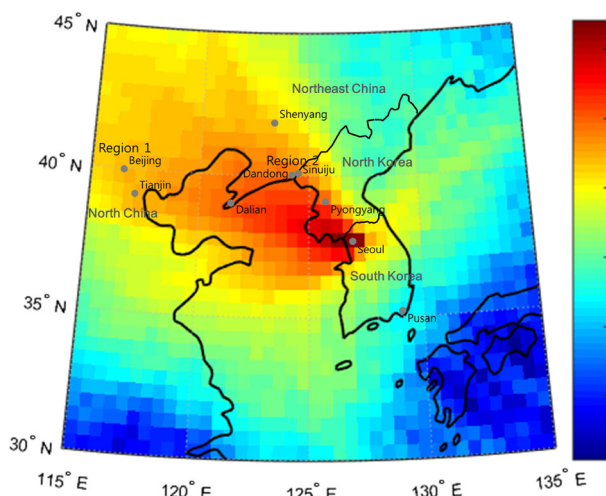
Fig. 2 Backward trajectory frequency during the sampling days between 2006 and 2007

Backward trajectory data

We performed backward trajectory analysis for the sampling days using the HYSPLIT4 (Hybrid single-particle lagrangian integrated trajectory) model (http://www.arl.noaa.gov/ready/hysplit4.html, NOAA Air Resources Laboratory, Silver Spring, MD, USA) with GDAS (Global Data Assimilation System, operated by the US National Weather Service's National Centers for Environmental Prediction) as the meteorological data. We calculated the trajectories at hourly intervals from 15:00 UTC when sampling started to 15:00 UTC the following day when sampling finished. For each sampling day between 2006 and 2007, we used six starting heights: 500, 1,000, 1,500, 2,000, 2,500, and 3,000 m. Given 73 sampling days, we mapped 10,950 trajectories to the PSCF.

When we carried out research on long-range transport of air pollutants from Siberia and Mongolia, 72 h (3 days) backward trajectories were insufficient for some sampling days. The
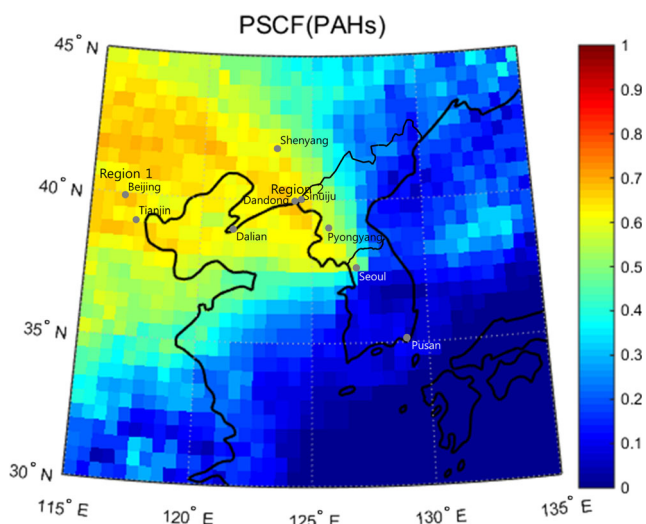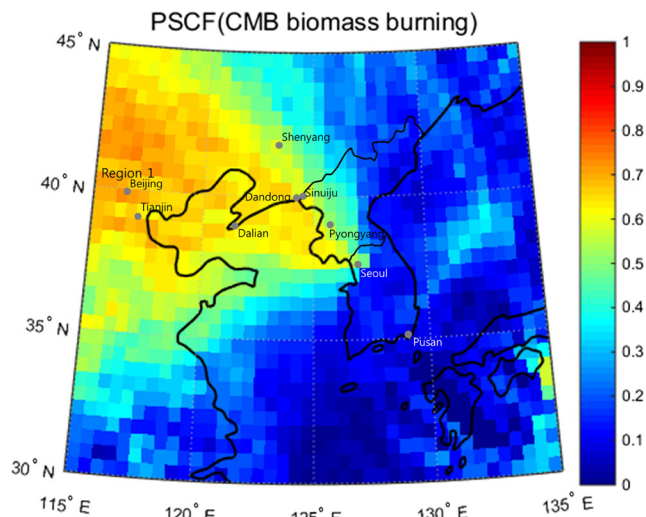

Fig. 3 PSCF plot of total particulate PAHs

Fig. 4 PSCF plot of particulate PAHs emitted from biomass burning calculated from the CMB modeling

backward trajectories during sampling days with slow wind speed covered only small parts of China and the Yellow Sea. Thus, to consider long- or middle-range transport of air pollutants, we set the duration time for these data to 120 h (5 days) in the backward trajectory analysis. Figure 2 shows the frequency with which backward trajectories passed through each grid cell on sampling days. Most air parcels traveled over North/Northeast China and passed over the Yellow Sea and then arrived at Seoul, though a few air parcels passed over Japan and East China during the sampling period.

Results and discussion

We applied total particulate PAH concentrations and the particulate PAH concentrations estimated to be from biomass burning to identify the variation of the major source area between 2D- and 3D-PSCF.

Figure 3 illustrates the 2D-PSCF result for the total particulate PAH concentrations observed at Seoul. Figure 4 shows the 2D-PSCF result for the particulate PAH concentrations estimated to be from biomass burning based on the CMB modeling result. The total particulate PAH concentration 2D-PSCF plot in Fig. 3 displays two major regions as probable primary contributors to high PAH levels in Seoul. The first region is over the northern part of Hebei Province, Beijing and Tianjin, China. The second region is the border area between Dandong, China, and Sinuiju, North Korea. On the other hand, as shown in Fig. 4, the PSCF values for particulate PAHs from biomass burning were high over the northern part of Hebei Province, Beijing and Tianjin, China.

Figures 5 and 6 show the 3D-PSCF values for total particulate PAHs and particulate PAHs from biomass burning, respectively, calculated with varying threshold heights. Figure 5
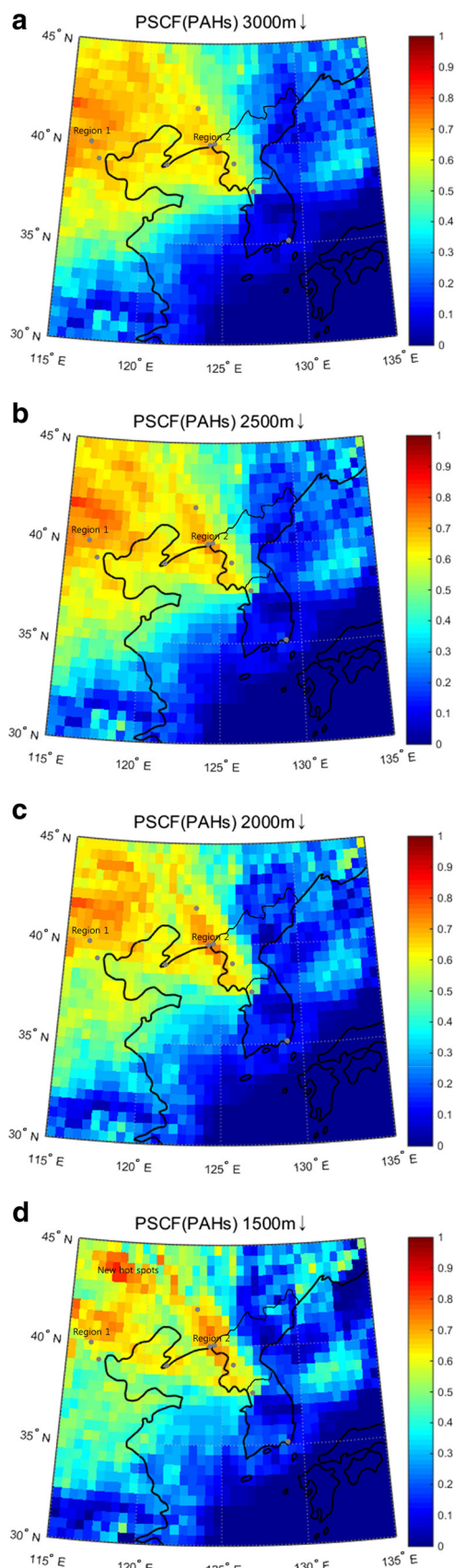
Fig. 5 PSCF plot of total particulate PAHs with varying threshold heights: **a** 3,000 m, **b** 2,500 m, **c** 2,000 m, **d** 1,500 m
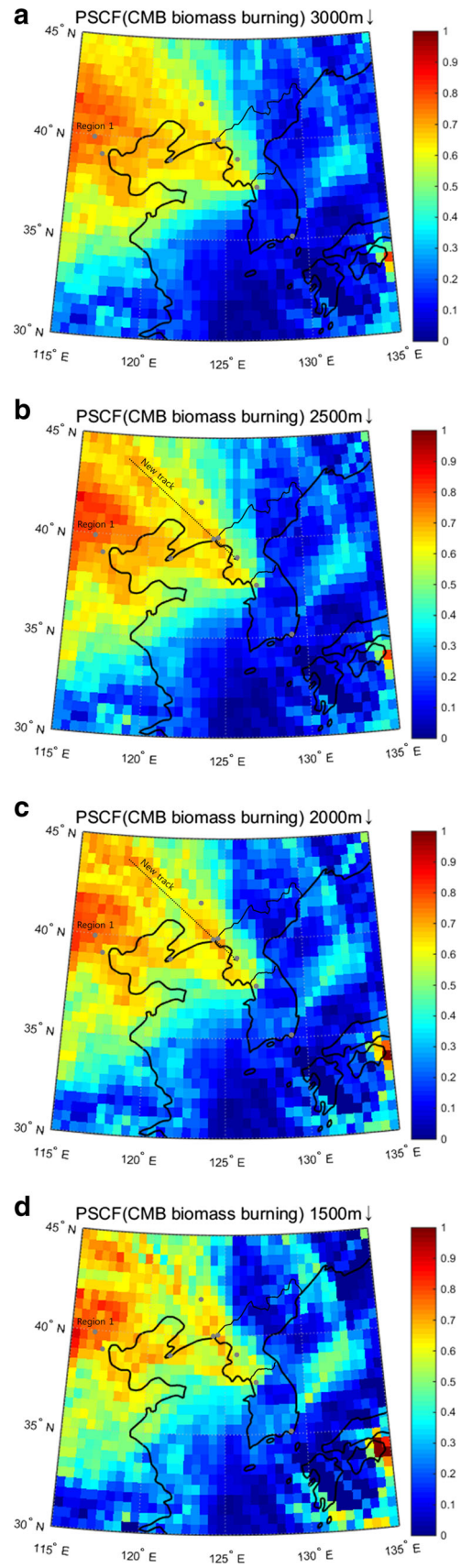
Fig. 6 PSCF plot of particulate PAHs from biomass burning with varying threshold heights: **a** 3,000 m, **b** 2,500 m, **c** 2,000 m, **d** 1,500 m

Table 2 The variation of the PSCF values between 2D- and 3D-PSCF

	2D-PSCF	3D-PSCF (threshold height)			
		3,000 m	2,500 m	2,000 m	1,500 m
Particulate PAHs	0.6661	0.7100	0.7073	0.6710	0.5810
Particulate (Figs. 3, 5) PAHs from biomass burning (Figs. 4, 6)	0.7223	0.7739	0.7840	0.7881	0.7432

confirms the major particulate PAH emission area as similar to that shown in Fig. 3; the north part of Hebei Province, Beijing, Tianjin and Dandong, Liaoning Province. As the threshold height decreases, however, hot spots appear more clearly at Beijing, the north part of Hebei, and the border area between Liaoning Province and North Korea. Figure 5 displays two main regions that contributed to the elevated concentration of particulate PAHs in Seoul. Region 1 started in the north part of Hebei Province and mainly appeared in Beijing; Region 2 appeared throughout the east part of Liaoning Province, China, and expanded to the border area between Dandong, China, and Sinuiju, North Korea. The two regions are most clearly shown in the PSCF plots with threshold heights of 2,000 m. On the contrary, at the threshold height of 1,500 m, the effects of particulate PAH emissions in Beijing was decreased and new hot spots appeared at Inner Mongolian region. 3D-method improved the ability of PSCF to indicate source location compared to 2D-method based on the value of PSCF. For example, the PSCF value at Beijing in Fig. 3 (using 2D-PSCF) was 0.6661. The values became higher, when threshold heights were lower in 3D-PSCF. However, when threshold height was 1,500 m, the value was lower than in 2D-PSCF due to the number of trajectories was too small to statistically meaningful result, as shown in Table 2. For the same reason, new hot spots appeared at Inner Mongolian region when threshold height was 1,500 m, in Fig. 5 (d), could be statistically meaningless. Still, with appropriate threshold height, 3D-PSCF identified major source area, such as Beijing, more clearly compare to 2D-PSCF.

Region 1 passed through high-energy-consumption areas in China. Coal consumption in Beijing, Tianjin, and Hebei Province was more than 9 % of the total coal consumption

in China between 2006 and 2007, as shown in Table 3. Liaoning Province consumed 4.6 % of all the coal in China between 2006 and 2007 (China NBS 2010) and contained major coal deposits and coal mines (IEA 1999). Therefore, northerlies or northwesterlies could transport a major fraction of particulate PAHs emitted from those areas to Seoul. The 3D-PSCF distinctly indicated the effects of emissions in Beijing, Tianjin, and Liaoning on particulate PAH concentrations in Seoul more clearly, as shown in Fig. 5, whereas 2D-PSCF evaluate the effect of those areas in low values and does not indicate the impact from Inner Mongolian region, as shown in Fig. 3.

In general, air pollutants emitted from the surface mix well in the boundary layer, 1–2 km. The mixing heights were generally less than 300 m under stable conditions and were in mixed-well conditions at 2–3 km in Seoul (Kim et al. 2007). In addition, the injection height of aerosols emitted from biomass burning varies with the conditions of burning, such as burning area, time, and materials (Mazzoni et al. 2007; Labonne et al. 2007; Freitas et al. 2007; Martin et al. 2010; Jian and Fu 2014). However, we considered that the limitation of injection heights for aerosols emitted by biomass burning was generally about 2 km. In this study, the effects in identifying the geographic location of an emission source using 3D-PSCF were noticeable below a height threshold of 2,000 m. However, when the threshold was lower than 1,500 m, PSCF values could be overestimated because of a decrease in the total number of trajectories used in the calculation.

Figure 6 illustrates the PSCF values for particulate PAHs from biomass burning with varying threshold heights. As the threshold heights decreased, the major source areas for particulate PAHs from biomass burning expanded over North China, such as Beijing and Hebei Province, which is indicated Region 1 in Fig. 6. We suggest that biomass burning in North China significantly influenced the air quality in Seoul because biomass burning occurred widely in North China. The emission of organic carbon (OC) from biomass burning in Northeast China (Heilongjiang Province and Jilin Province), located right above North Korea, was 27.5 % of the total OC emissions from biomass burning throughout China (Streets et al. 2003). However, PSCF values for particulate PAHs emitted from biomass burning appear high over North China (i.e.,

Table 3 Coal consumption in China by region (unit, 10,000 tonne) (China NBS 2010)

Region	2000		2005		2006		2007		2008		2009	
Beijing	2,720	(1.9 %)	3,069	(1.2 %)	3,056	(1.0 %)	2,985	(0.9 %)	2,748	(0.8 %)	2,665	(0.8 %)
Tianjin	2,473	(1.7 %)	3,801	(1.4 %)	3,809	(1.3 %)	3,927	(1.2 %)	3,973	(1.2 %)	4,120	(1.2 %)
Hebei	12,115	(8.2 %)	20,542	(7.7 %)	21,360	(7.1 %)	24,681	(7.7 %)	24,419	(7.3 %)	26,516	(7.6 %)
Liaoning	9,582	(6.5 %)	12,710	(4.8 %)	13,837	(4.6 %)	14,712	(4.6 %)	15,347	(4.6 %)	16,033	(4.6 %)
Shandong	8,698	(5.9 %)	26,056	(9.8 %)	29,838	(10.0 %)	32,719	(10.2 %)	34,390	(10.3 %)	34,795	(9.9 %)
Total	146,921		265,473		299,099		321,126		334,806		351,182	

Beijing, Tianjin, Hebei, and part of Shandong) in Fig. 6, possibly because PAH emissions from biomass burning and biofuel consumption were larger in North China than in Northeast China (Zhang and Tao 2008). Compared to the result of the conventional PSCF, Region 1 is clearly displayed in the results with 2,500 and 2,000 m thresholds in Fig. 6. Furthermore, a new track appeared from the north. When applying a 1,500 m threshold, the possible source areas appear quite fragmented, and the track is not apparent. Based on the results of Figs. 5 and 6, 2,000 m height is an appropriate threshold height in 3D-PSCF to find source area for residential biomass burning and small open burning. The PSCF values in Table 2 also confirms this result.

Whereas the PSCF values over China vary considerably between the 3D-PSCF and the conventional 2D-PSCF, we did not observe a similar change over North Korea. However, PSCF values over Pyongyang and the west part of North Korea gradually became noticeable from those of surrounding areas as the threshold heights decreased. Pyongyang, the capital of North Korea, has approximately 13.6 % of the total population in North Korea and is the country's center of industry, economy, and transportation (UNEP 2012). Therefore, energy consumption in Pyongyang including biofuel might be larger than in the surrounding area. Differences in air pollutant emissions inside North Korea were thus distinguished in 3D-PSCF, whereas the 2D-PSCF did not show a higher value over Pyongyang.

Conclusion and further study direction

We developed 3D-PSCF to apply injection heights to the PSCF calculation. As sources for high particulate PAH concentrations in Seoul, 3D-PSCF clearly distinguished the mega-source areas, Beijing, Tianjin, and Liaoning, especially at 2,000 m, unlike 2D-PSCF. The high potential source areas for biomass fuel burning estimated by 3D-PSCF were including Pyongyang, North Korea, which did not appear in the 2D-PSCF results. Lee and Kim (2007) and Kim et al. (2013) evaluated North Korea as a source area of particulate PAHs in Seoul emitted by biomass burning between 2002 and 2003. Using PSCF calculations with threshold heights allowed us to identify the geographical position of large source area, big cities using biomass for fuel.

Nonetheless, this study has some limitations. Statistical errors could occur in the PSCF calculations. We did not use the arbitrary weight function often used in other PSCF calculations to reduce the values of cells with few endpoints. Those kinds of statistical errors could be reduced by using more sampling data. In future work, we will add ambient data from between 2010 and 2011. In addition, the inherent uncertainty of CMB results could affect understanding of the source of biomass fuel burning in the 3D-PSCF calculation. The use of

another biomass key marker, such as levoglucosan (1,6-anhydro-b-D-glucopyranose), could reduce that uncertainty. The work would support the research for quantifying the impact of air pollutants emitted from biomass fuel burning in North Korea to air quality in Seoul.

References

Ashbaugh LL, Malm WC, Sadeh WZ (1985) A residence time probability analysis of sulfur concentrations at grand canyon national park. Atmos Environ 19:1263–1270

Cheng, M. D., Hopke, P. K., Zeng Y. (1993a) A receptor-oriented methodology for determining source regions of particle sulfate composition observed at Dorset, Ontario. J Geophys Res, 98, 16839-16849

Cheng, M. D., Hopke, P. K., Barrie, L., Rippe, A., Olson, M., Landsberger S. (1993b) Qualitative determination of source regions of aerosol in Canadian high Arctic. Environ Sci Technol, 27, 2063-2071

Cheng MD, Gao N, Hopke PK (1996) Source apportionment study of nitrogen species measured in Southern California in 1987. J Environ Eng 122:183–190

China NBS, China National Bureau of Statistics (2010) China Energy Statistical Yearbook 2009

Choi H, Zhang YH, Kim KH (2008) Sudden high concentration of TSP affected by atmospheric boundary layer in Seoul metropolitan area during duststorm period. Environ Int 34:635–647

Fan A, Hopke PK, Raunemaa RM, Öblad M, Pacyna JM (1995) A study on the potential sources of air pollutants observed at Tjörn, Sweden. Environ Sci Pollut Res 2(2):107–115

Freitas SR, Longo KM, Chatfield R, Latham D, Silva Dias MAF, Andreae MO, Prins E, Santos JC, Gielow R, Carvalho JA Jr (2007) Including the sub-grid scale plume rise of vegetation fires in low resolution atmospheric transport models. Atmos Chem Phys 7:3385–3398

Gao N, Cheng MD, Hopke PK (1993) Potential source contribution function analysis and source apportionment of sulfur species measured at Rubidoux, CA during the southern California air quality study, 1987. Anal Chim Acta 277:369–380

Gao N, Cheng MD, Hopke PK (1994) Receptor modeling of airborne ionic species collected in SCAQS, 1987. Atmos Environ 28:1447–1470

Gao N, Hopke PK, Reid NW (1996) Possible sources of some trace elements found in airborne particles and precipitation in Dorset, Ontario. J Air Waste Manag Assoc 46:1035–1047

Heo JB, Hopke PK, Yi SM (2009) Source apportionment of PM2.5 in Seoul, Korea. Atmos Chem Physics 9:4957–4971

Hopke PK, Gao N, Cheng MD (1993) Combining chemical and meteorological data to infer source areas of airborne pollutants. Chemometrics Intelligent Lab Syst 19(2):187–199

Hopke PK, Barrie LA, Li S-M, Cheng M-D, Li C, Xie Y (1995) Possible sources and preferred pathways for biogenic and non-sea-salt sulfur for the high Arctic. J Geophys Res 100:16595–16603

IEA, International Energy Agency (1999) Coal in the energy supply of China- Report of the CIAB Asia Committee, Coal Industry Advisory Board, IEA

In HJ, Kim YP (2010) Estimation of the aerosol optical thickness distribution in the Northeast Asian forest fire episode in May 2003: possible missing emissions. Atmos Res 98:261–273

Jian Y, Fu TM (2014) Injection heights of springtime biomass-burning plumes over peninsular Southeast Asia and their impacts on long-range pollutant transport. Atmos Chem Phys 14:3977–3989

Jung DB, Cho YS, Kim IS, Lee JY, Kim YP (2015) Impact of energy consumption in Northeast Asia to the particulate PAHs levels and composition at Seoul. Aerosol Air Qual Res 15(6):2190–2199

Kim SW, Yoon SC, Won JG, Choi SC (2007) Ground-based remote sensing measurements of aerosol and ozone in an urban area: a case study of mixing height evolution and its effect on ground-level ozone concentrations. Atmos Environ 41:7069–7081

Kim IS, Lee JY, Kim YP (2013) Impact of polycyclic aromatic hydrocarbon (PAH) emissions from North Korea to the air quality in the Seoul Metropolitan Area, South Korea. Atmos Environ 70:159–165

Labonne M, Bréon F, Chevallier F (2007) Injection height of biomass burning aerosols as seen from a spaceborne lidar. Geophsical Res Lett 34:L11806. doi:10.1029/2007GL029311

Lee JY, Kim YP (2007) Source apportionment of the particulate PAHs in Seoul, Korea: impact of long range transport to a megacity. Atmos Chem Phys 7:3587–3596

Lee JY, Kim YP, Kang CH (2011) Characteristics of the ambient particulate PAHs in Seoul, a mega city of Northeast Asia in comparison with the characteristics of a background site. Atmos Res 99:50–56

Li A, Jang JK, Scheff PA (2003) Application of EPA CMB8.2 model for source apportionment of sediment PAHs in Lake Calumet, Chicago. Environ Sci Technol 37:2958–2965

Nguyen DL, Kim JY, Ghim YS, Shim SG (2015) Influence of regional biomass burning on the highly elevated organic carbon concentrations observed at Gosan, South Korea during a strong Asian dust period. Environ Sci Pollut Res 22(5):3594–3605

Malm WC, Johnson CE, Bresch JF (1986) Application of principal component analysis for purposes of identifying source-receptor relationships. In: Pace TG (ed) receptor methods for source apportionment. Air Pollution Control Association, Pittsburgh, PA, pp 127–148

Marr LC, Dzepina K, Jimenez JL, Reisen F, Bethel HL, Arey J, Gaffney JS, Marley NA, Molina LT, Molina MJ (2006) Sources and transformations of particle-bound polycyclic aromatic hydrocarbons in Mexico City. Atmos Chem Phys 6:1733–1745

Martin MV, Logan JA, Kahn RA, Leung FY, Nelson DL, Diner DJ (2010) Smoke injection heights from fires in North America: analysis of 5 years of satellite observations. Atmos Chem Phys 10:1491–1510

Mazzoni D, Logan JA, Diner D, Kahn R, Tong L, Li Q (2007) A data-mining approach to associating MISR smoke plume heights with MODIS fire measurements. Remote Sens Environ 107:138–148

Ravindra K, Sokhia R, Griekenb RV (2008) Atmospheric polycyclic aromatic hydrocarbons: source attribution, emission factors and regulation. Atmos Environ 42(13):2895–2921

Rogge WF, Hidlemann LM, Mazurek MA, Cass GR, Simoneit BRT, (1993a) Sources of fine organic aerosol. 2. Noncatalyst and catalyst-equipped automobiles and heavy duty diesel trucks. Environ Sci Tech 27:636–651

Rogge WF, Hidlemann LM, Mazurek MA, Cass GR, Simoneit BRT (1993b) Sources of fine organic aerosol. 5. Natural gas home appliances. Environ Sci Tech 27:2736–2744

Rogge WF, Hidlemann LM, Mazurek MA, Cass GR (1998) Sources of fine organic aerosol. 9. Pine, oak, and synthetic log combustion in residential fireplaces. Environ Sci Tech 32:13–22

Stohl A (1998) Computation, accuracy and applications of trajectories—a review and bibliography. Atmos Environ 32(6):947–966

Streets DG, Bond TC, Carmichael GR, Fernandes SD, Fu Q, He D, Klimont Z, Nelson SM, Tsai NY, Wang MQ, Woo J-H, Yarber KF (2003) An inventory of gaseous and primary aerosol emissions in Asia in the year 2000. J Geophys Res 108(D21):8809

Streets DG, Yarber KF (2003) Biomass burning in Asia: annual and seasonal estimates and atmospheric emissions. Global Biogeochem Cycles 17(4):1099. doi:10.1029/2003GB002040

Tian YZ, Shi GL, Han B, Wua JH, Zhou XY, Zhou LD, Zhang P, Feng YC (2015) Using an improved Source Directional Apportionment method to quantify the PM2.5 source contributions from various directions in a megacity in China. Chemosphere 119:750–756

Tian YZ, Chen G, Wang HT, Huang-Fu YQ, Shi GL, Han B, Feng YC (2016) Source regional contributions to PM2.5 in a megacity in China using an advanced source regional apportionment method. Chemosphere 147:256–263

UNEP (United Nations Environment Programme) (2012) Democratic People's Republic of KOREA - Environment and Climate Change Outlook, Pyongyang 2012, ISBN: 978-9946-1-0170-5

Venturini E, Vassura I, Raffo S, Ferroni L, Bernardi E, Passarini F (2014) Source apportionment and location by selective wind sampling and Positive Matrix Factorization. Environ Sci Pollut Res 21(20): 11634–11648

Wallace, J. M. and P. V. Hobbs (2006) Atmospheric science: an introductory survey, Academic Press, ISBN: 9780127329512

Wang YQ, Zhang XY, Arimoto R, Cao JJ, Shen ZX (2004) The transport pathways and sources of PM10 pollution in Beijing during spring 2001, 2002 and 2003. Geophys Res Lett 31:L14110

Wang YQ, Zhang XY, Arimoto R (2006) The contribution from distant dust sources to the atmospheric particulate matter loadings at XiAn, China during spring. Sci Total Environ 368:875–883

Zeng Y, Hopke PK (1989) A study on the sources of acid precipitation in Ontario, Canada. Atmos Environ 23:1499–1509

Zhang Y, Tao S (2008) Seasonal variation of polycyclic aromatic hydrocarbons (PAHs) emissions in China. Environ Pollut 156:657–663

Zhang YF, Xu H, Tian YZ, Shi GL, Zeng F, Wu JH, Zhang XY, Li X, Zhu T, Feng YC (2011) The study on vertical variability of PM10 and the possible sources on a 220 m tower, in Tianjin, China. Atmos Environ 45:6133–6140